Available online at www.sciencedirect.com
ScienceDirect
Procedia Engineering 62 (2013) 202 – 210
Procedia Engineering
www.elsevier.com/locate/procedia

The 9th Asia-Oceania Symposium on Fire Science and Technology

Facade flame heights from enclosure fires with side walls at the opening

Kaihua Lu[a], Longhua Hu[a,]*, Fei Tang[a], Michael Delichatsios[b], Xiaochun Zhang[a], Linghui He[a]

[a]State Key Laboratory of Fire Science,University of Science and Technology of China, Hefei 230026, China
[b]FireSERT, School of Built Environment and Built Environment Research Institute, University of Ulster, Newtownabbey, BT38 8GQ, Northern Ireland

Abstract

This paper presents an investigation of facade flame heights from an under-ventilated enclosure fire having an opening with side walls. A reduced-scale model, consisting of a cubic enclosure of 0.4 m with a vertical facade wall and two side walls was constructed for the experiments. The temperature profile inside the enclosure was measured by thermocouples whereas a CCD camera was employed to obtain the mean flame height of the ejected flames. It is found that the presence or the separation distance of the side walls have no impact on the critical heat release rate of the enclosure ($1500A\sqrt{H}$ in kW). The effects of the side walls on the mean flame height are pronounced for a relative larger flame than a small one having the same separation distance of the side walls. In addition as the side wall distance decreases, the effects become larger leading to flame heights much higher than those without sidewalls. A global dimensionless parameter *K* is proposed to account for the side wall effects, based characteristic length scales of the opening , and the distance between the side walls *D*. The experimental data for different opening dimensions and side wall distances are well correlated by this global parameter.

Selection and peer-review under responsibility of the Asian-Oceania Association of Fire Science and Technology

Keywords: Enclosure fire; Side wall; Mean flame height

Nomenclature

g	acceleration of gravity (m/s^2)
h_c	total heat loss coefficient from enclosure (kW/m^2/K)
$\dot{m}_a$	mass flow rate of air supply (kg/s)
$\dot{m}_f$	mass flow rate of fuel (kg/s)
A	area of the opening (m^2)
A_T	total exposed surface area of the enclosure (m^2)
$A\sqrt{H}$	ventilation factor (m$^{2.5}$)
C_p	specific heat (kJ/kg/K)
D	distance of the two side walls (m)
K	global parameter of mean flame height
H	height of the opening (m)
ΔH	heat of combustion of the gas fuel (kW/m^3)
ΔH_{ox}	heat release per mass of air consumed at normal conditions (3000 kJ/kg)
$\dot{Q}$	heat release rate (kW)

* Corresponding author. Tel.: +86 551 6360 6452; fax: +86 551 6360 1669.
E-mail address: hlh@ustc.edu.cn.

Selection and peer-review under responsibility of the Asian-Oceania Association of Fire Science and Technology
doi:10.1016/j.proeng.2013.08.056

$\dot{Q}_{ex}$	excess heat release rate, $\dot{Q}_{ex} = \dot{Q} - \dot{Q}_{inside}$ (kW)
$\dot{Q}_{ex}^*$	non-dimensional excess heat release rate, $\dot{Q}_{ex}^* = \dfrac{\dot{Q}_{ex}}{\rho_\infty c_p T_\infty \sqrt{g} \ell_1^{5/2}}$
$\dot{Q}_{inside}$	heat release rate inside the compartment (kW)
T_∞	ambient temperature (K)
$\dot{V}$	volume flow rate (m^3/h)
W	width of the opening (m)
Z_0	mean flame height without side walls (m)
Z_D	mean flame height with side walls at distance of *D* (m)
Z_n	location of the neutral plane (m)
Greek symbols	
ℓ_1	characteristic length scale, $\ell_1 = (A\sqrt{H})^{2/5}$ (m)
ℓ_2	characteristic length scale, $\ell_2 = (AH^2)^{1/4}$ (m)
λ	coefficient to describe the difference of entrainment strength from side with that from front
ρ_f	density of fuel (kg/m^3)
ρ_∞	density of air (kg/m^3)
Subscripts	
a	air
f	fuel
∞	ambient condition

1. Introduction

When a fire occurs in a high rise building, there is a threat that fire can spread to upper floors from the openings. Typically, flame spread to the upper floors is mainly due to radiation and convection of the flames on the facade which are determined by two important parameters, i.e. the flame height and the temperature profile of the ejected spill plume. Started by Yokoi [1] in 1960, several investigators [2-11] have studied enclosure fire behaviour, including the spill flames and plumes. Enclosure fires can be divided into two regimes, the fuel-controlled and the ventilation-controlled regime. The transition from over to under ventilated condition depends on the fuel supply rate inside compared to the air supply rate into the enclosure. The air supply rate depends on $A\sqrt{H}$, also known as the ventilation factor of an opening [12], where *A* (m^2) and *H* (m) represent the area and height of the opening respectively. For under-ventilated conditions the air supply rate is:

$$\dot{m}_a = 0.133 \rho_\infty A \sqrt{gH} = 0.5 A\sqrt{H} \text{ in kg/s} \tag{1}$$

Recently this relation has been verified from a series of small-scaled experiments and analysis in a 0.5 m cubic enclosure [13-17, 28]. In addition the heat release rate inside the enclosure for under-ventilated conditions is determined by [13-17, 28]:

$$\dot{m}_a \Delta H_{ox} = 0.133 \frac{\Delta H_{ox}}{c_p T_\infty} c_p T_\infty \rho_\infty A\sqrt{gH} = 3000 \times 0.5 A\sqrt{H} = 1500 A\sqrt{H} \text{ in kW} \tag{2}$$

where ΔH_{ox} is the heat released per mass of air consumed in the enclosure.

When the theoretical heat release rate from the fuel supplied in the enclosure exceeds the critical value in Eq. (2), the excess fuel burns outside the enclosure creating the facade flames. In this case, the mean height of spill flames is determined by two factors: the amount of excess fuel and the opening of the enclosure [13, 16]. A non-dimensional parameter $\dot{Q}_{ex}^*$ was introduced [13, 16], on which the mean flame height depends as:

$$\frac{Z_f - Z_n}{\ell_1} = f(\dot{Q}_{ex}^*) = f\left(\frac{\dot{Q}_{ex}}{\rho_\infty C_p T_\infty \sqrt{g} \ell_1^{5/2}}\right) \tag{3}$$

$$\ell_1 = (A\sqrt{H})^{2/5} \tag{4}$$

where Z_f is the mean (50% intermittency) flame height, Z_n is the location of the neutral plane, ρ_∞ is air density, C_p is specific heat of air at constant pressure, T_∞ is ambient temperature, g is acceleration of gravity, ℓ_1 is the characteristic length scale describing the opening size. $\dot{Q}^*_{ex}$ is the excess heat release rate due to the burning excess fuel outside the compartment defined as:

$$\dot{Q}_{ex} = \dot{Q} - \dot{Q}_{inside} \tag{5}$$

Eqs. (3) - (5) are valid on plain facades. Additional experiments have been reported on ejected flames on facades with horizontal eaves or a facing wall [18, 19-24, 28]. However, little work has been reported on the effects of sidewalls on temperatures in facade flames [23] but none on flame heights.

In this paper, a series of experiments were conducted in a small cubic enclosure of size 0.4 m having two side walls on both sides of the opening. By changing the distance of the side walls, we measured the flame heights for different opening conditions using a CCD camera. In addition, the temperature profile was measured by thermocouples trees. A global coefficient was found to account for the side wall effect including the characteristic length scales of the opening and the side wall separation distance.

There are three more sections following the introduction. The second section describes the experimental procedure, devices, equipment and conditions. The third section includes the results and discussions and finally section four summarizes the conclusions.

2. Experimental setup and procedure

2.1. Experimental rig

Figure 1 shows a reduced-scale model, consisting of a cubic enclosure with a vertical facade wall and two side walls. The enclosure is a 0.4 m cube with a 0.05 m thick inner lining of ceramic fibre boards for thermal insulation. The bottom of the enclosure is at a height 0.3 m from the ground. The facade wall is 1 m wide and 2.2 m high covered by a fire resisting board 5 mm thick. The two side walls also made of fire resisting board, 0.6 m wide and 2.1 m high, are positioned symmetrically at both sides of the opening at distances varying from 0.30 m to 0.75 m with 0.15 m increment.

The opening is located in the centre of the facade wall of the enclosure. Five kinds of windows are used in the experiments to represent different ventilation conditions and the specific opening geometries are also listed in Fig. 1. A square porous gas burner of 0.2 m welded by steel plates of thickness 2 cm is employed to provide the fuel supply into the enclosure. Small holes of diameters 0.5 cm have been drilled within a square region on the top surface of the gas burner at a spacing of 2 cm to stabilize the fuel supply into the enclosure.

2.2. Measurement and experimental conditions

We use Liquefied Petroleum Gas (LPG) as fuel. A gas flow meter of accuracy 0.1 m^3/h monitors and controls the gas fuel supply rate $\dot{V}_f$. All these conditions correspond to under-ventilated fires. The total heat release rates calculated from Eq. (6) are listed in Table 1:

$$\dot{Q} = \rho_f \dot{V}_f \Delta H \tag{6}$$

where ρ_f is density of fuel, and ΔH is heat of combustion of the gas fuel.

A total of 8 K-type thermocouples of diameter 0.5 mm are divided in two groups located at the inner and outer corners of the enclosure respectively (see Fig. 1). The thermocouples in each thermocouple tree are 0.2 m, 0.25 m, 0.3 m and 0.35 m from the bottom of the enclosure. In each scenario when the combustion inside the enclosure reaches a steady state, the vertical temperature distribution is recorded every 120 seconds.

A CCD camera (at 25 frames per second) records the fluctuations of the ejected flames. The distance from the camera to the facade wall is maintained at 3 m in the experiments. The mean flame heights are acquired through image processing. The experimental scenarios are summarized in Table 1 for the opening sizes, the distances of the side walls, the volume flow rates of fuel and the total heat release rate.

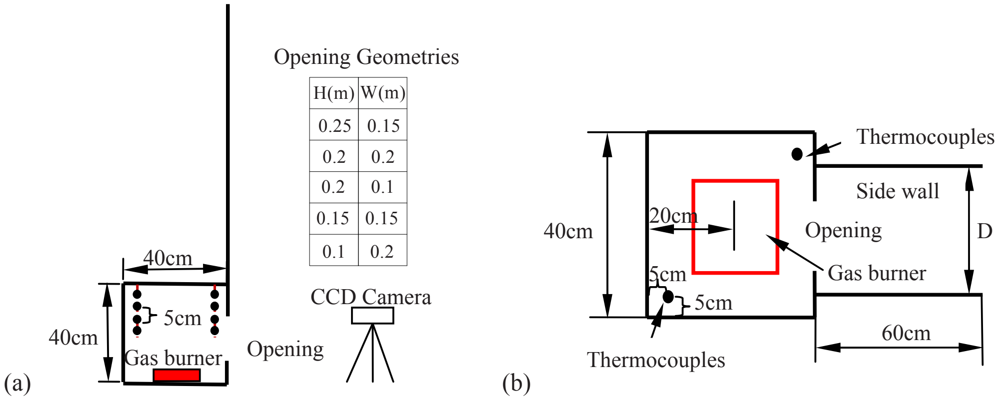

Fig. 1. Schematic of experimental rig: (a) side view; (b) top view.

Table 1. Summary of experimental scenarios

Test Series.	Opening geometry		Separation Distance of side walls (m)					Total heat release rate (kW)		
	Height (m)	Width (m)								
1	0.25	0.15	0.3	0.45	0.6	0.75	No side walls	39.90	44.34	48.77
2	0.2	0.2	0.3	0.45	0.6	0.75	No side walls	39.90	44.34	48.77
3	0.2	0.1	0.3	0.45	0.6	0.75	No side walls	39.90	44.34	48.77
4	0.15	0.15	0.3	0.45	0.6	0.75	No side walls	39.90	44.34	48.77
5	0.1	0.2	0.3	0.45	0.6	0.75	No side walls	39.90	44.34	48.77

3. Results and discussion

3.1. Temperature inside the enclosure

Figure 2 shows the inside temperature distribution for a typical opening (0.15 m × 0.15 m) for all side wall separation distances. It is seen that the temperature inside the enclosure is spatially uniform, ranging from about 650 °C to about 750 °C. In addition, the temperatures inside are nearly the same for varying total heat release rates but the same opening. According to the energy balance [14], the gas temperature rise ΔT_g inside the enclosure can be expressed as:

$$0.133\frac{\Delta H_{ox}}{C_p T_\infty} C_p T_\infty \rho_\infty A\sqrt{gH} = 1500A\sqrt{H} = \dot{Q}_{inside} = (\dot{m}_f + \dot{m}_a)C_p \Delta T_g + h_c A_T \Delta T_g \quad (7)$$

$$\dot{m}_a \gg \dot{m}_f \quad \text{(the mass flow rate of fuel)} \quad (8)$$

where h_c is the heat loss coefficient from the walls and the opening of the enclosure, A_T is the total exposed surface area of the enclosure. It can be concluded from Fig. 2 and Eq. (7) that the presence or the distance of side walls have no influence on the critical heat release rate ($1500A\sqrt{H}$, in kW) at a certain opening geometry.

3.2. Mean flame height

In the experiments, the mean flame height was obtained by a series of continuous images recorded by the CCD camera at a speed of 25 frames per second. The OTSU method [29] was applied to obtain the flame height. The mean flame height is obtained where the intermittency is 0.5.

On the basis of [11, 14, 26], two physical mechanisms dominate the mean flame height into different stages. For small flames of $\dot{Q}_{ex}^{*} \leq 1.3$, the entrainment of air mostly occurs from front of the opening and the flame is attached to the facade wall. Otherwise, for large flames of $\dot{Q}_{ex}^{*} > 1.3$ the increase of entrainment from side of the opening will make the flame behaviour become more similar to axisymmetric fires.

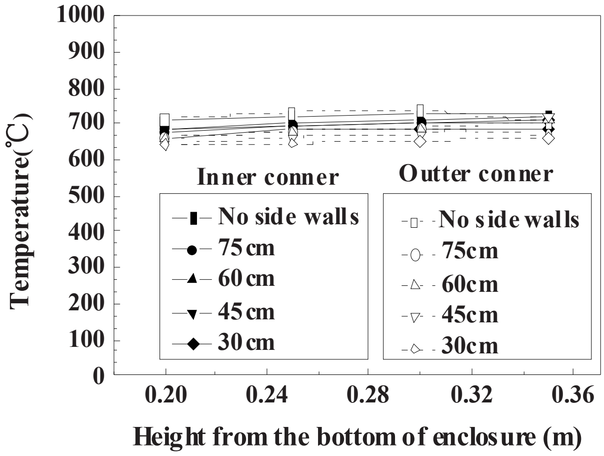

Fig. 2. Vertical temperature distribution of a typical opening (0.15 m × 0.15 m) with all side walls inside the enclosure: HRR= 48.77 kW.

Figure 3 shows the mean flame height with different side wall constrains under different heat release rates and openings. In the two big openings where $\dot{Q}_{ex}^{*}$ is relatively small, the mean flame height seems less depended on the distance of side walls, shown in Fig. 3(a) and Fig. 3(b). The mean flame height is almost consistent with different side wall constrains because of the entrainment is mainly come from the front. However, in small openings, such as Fig. 3(c) – Fig. 3(e), the impact of side walls is clearer, especially when the heat release rate is increased. This is because the presence of the side walls will strongly restrict air entrainment from the side. With the narrow down of the distance of side walls, the effect becomes more and more crucial and the mean flame height is much higher than that of free condition.

3.3. Correlation of the mean flame height under side wall constrains and dimensionless excess heat release rate

It is found that the dimensionless excess heat release and the distance of side walls are two major factors under side wall constrains. As stated above, for a small dimensionless excess heat release $\dot{Q}_{ex}^{*}$, the mean flame height has little dependence on the distance of side walls, so in this section we are mainly focused on relatively large flames (for $\dot{Q}_{ex}^{*}>1.3$) under side wall constrains. We introduce a global dimensionless parameter *K* to describe the mean flame height in such conditions:

$$\frac{Z_D}{\ell_1} = K \cdot \frac{Z_0}{\ell_1} \tag{9}$$

where Z_0 is the mean flame height without side walls and Z_D is the mean flame height with side wall distance of *D*.

According to some former studies [16], the flow outside the enclosure can be depicted as generated by a rectangular burner having sides ℓ_1 and ℓ_2 at the level of the neutral plane and providing a heat release rate of $\dot{Q}_{ex}$, where ℓ_2 describes the competition of momentum and buoyancy flux at the opening for the case of under ventilated fire condition. We suppose the coefficient *K* as a function of these two characteristic length scales:

$$K = f(D, \ell_1, \ell_2) \tag{10}$$

ℓ_1 is defined by Eq. (4) mentioned above, and ℓ_2 is defined as: $\ell_2 = (AH^2)^{1/4}$.

It is known that the flame ejecting behaviour is closely related to the air entrainment from surroundings. When the hot unburned fuel is ejected from the opening and move upwards, it will not come to flames until the mixing of fresh air is sufficient to support combustion, which means that the mean flame height has a negative correlation with the entrainment of fresh air. We can estimate relative values of the entrainment from front and from side by assuming that the entrainment is proportional to its characteristic length scale respectively. For an open space without side walls, entrainment occurs from three sides of the rectangular of length ℓ_1 and ℓ_2 and the relative entrainment length scale is supposed to be $\ell_1 + 2\lambda\ell_2$. For another extreme condition that the distance of side walls is ℓ_1 where the entrainment from side is fully constrained, the total entrainment amount takes only a length scale of ℓ_1. Here λ is introduced as a coefficient to describe the difference of entrainment strength from side with that from front.

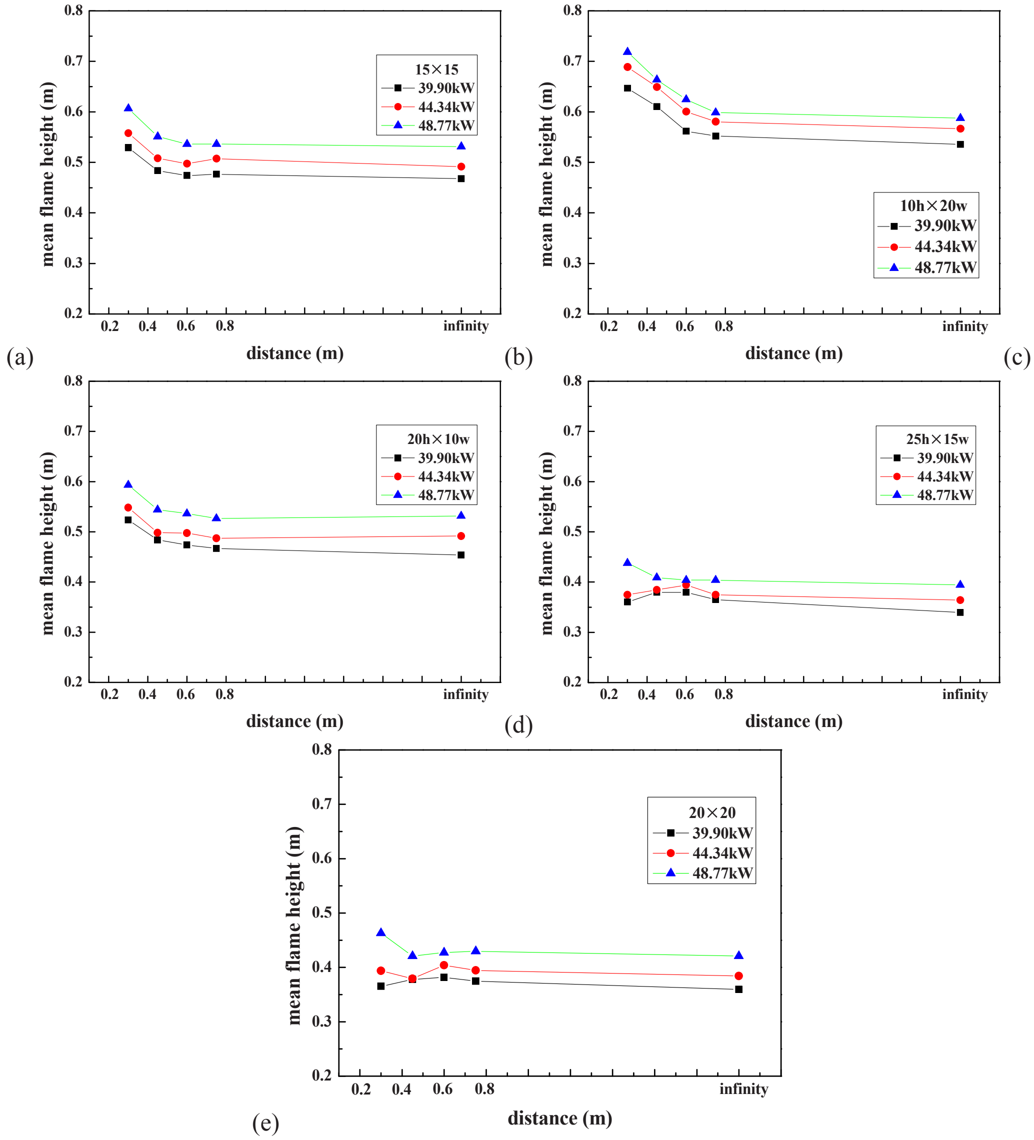

Fig. 3. The mean flame height versus different side walls distances in various opening geometries: (a) 0.15 m × 0.15 m; (b) 0.10 m (h) × 0.20 m (w); (c) 0.20 m (h) × 0.10 m (w); (d) 0.25 m (h) × 0.15 m (w); (e) 0.20 m × 0.20 m.

Then, based on above considerations, as the entrainment from side occurs when the separation distance of side walls increases, another dimensionless parameter $1 + 2\lambda(\frac{\ell_2}{\ell_1} - \frac{\ell_2}{D})$, integrated by the distance of side walls as well as two characteristic length scales is proposed to modify the entrainment length scale as $\ell_1 \cdot [1 + 2\lambda(\frac{\ell_2}{\ell_1} - \frac{\ell_2}{D})]$, and thus the parameter K is expressed as:

$$K = \frac{Z_D}{Z_0} = \{\frac{\ell_1 \cdot [1 + 2\lambda(\ell_2/\ell_1 - \ell_2/D)]}{\ell_1 + 2\lambda\ell_2}\}^{-1} = \frac{\ell_1 + 2\lambda\ell_2}{\ell_1 \cdot [1 + 2\lambda(\frac{\ell_2}{\ell_1} - \frac{\ell_2}{D})]} \tag{11}$$

Here when the distance of side walls ranges from ℓ_1 to infinity (equals to open space), the parameter K is valued from $\frac{\ell_1}{\ell_1 + 2\lambda\ell_2}$ to 1, corresponding to the two extreme conditions. Assumingly taking $\lambda = 0.2$, the experimental data are presented in Fig. 4. It is shown that the experimental data are shown to be well collapsed with this global parameter, suggesting following expression for K:

$$\frac{\ell_1 + 0.4\ell_2}{\ell_1 \cdot [1 + 0.4(\frac{\ell_2}{\ell_1} - \frac{\ell_2}{D})]} \quad \text{For } \dot{Q}_{ex}^* > 1.3 \tag{12}$$

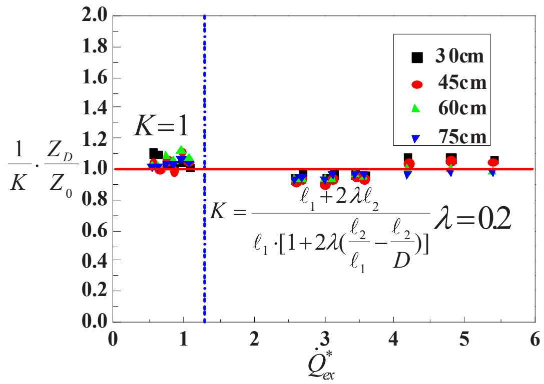

Fig. 4. Correlation of the global parameter K and the mean flame height with dimensionless excess heat release rate.

And also the mean flame height with side walls can be approximated by the following expressions:

$$\frac{Z_D}{\ell_1} = K \cdot \frac{Z_0}{\ell_1} = K \cdot \frac{f(\dot{Q}_{ex}^*)}{\ell_1} \tag{13}$$

$$K = \begin{cases} 1 & \dot{Q}_{ex}^* \le 1.3 \\ \frac{\ell_1 + 0.4\ell_2}{\ell_1 \cdot [1 + 0.4(\frac{\ell_2}{\ell_1} - \frac{\ell_2}{D})]} & \dot{Q}_{ex}^* > 1.3 \end{cases} \tag{14}$$

However, it should be noted in Fig. 4 that these seems to be still a small dependency of λ and thus the parameter K with ($\dot{Q}_{ex}^*$ >1.3), the value of λ is shown to be higher when $\dot{Q}_{ex}^*$ is larger. When $\dot{Q}_{ex}^*$ is large enough, the facade flame entrainment behaviors similarly to that of an axis-symmetrical free fire plume and thus the value of λ should approach unity.

4. Conclusions

This paper studies the flame ejecting behavior of enclosure fires under side wall constrains through a reduced-scale model experiments. The distance of the side walls is changed and the temperature profile inside the enclosure and the mean flame height of ejected flames are obtained to study the influence of side walls. The major findings are concluded through analysis and discussion:

(1) The temperature inside the enclosure is spatially uniform and almost the same for various total heat release rates but the same opening. The appearance or the distance of side wall has no influence on the critical heat release rate ($1500A\sqrt{H}$, in kW) at a certain opening geometry.

(2) For a small flame ($\dot{Q}_{ex}^{*} \leq 1.3$), the mean flame height has little dependence on the side walls, but for a relative larger flame ($\dot{Q}_{ex}^{*} > 1.3$), with the narrow down of the distance of side walls, the influence becomes more and more crucial and the mean flame height is much higher than that of free condition, dues to a severe constrain of the entrainment from side.

(3) A global parameter K (Eq. (14)) is founded to predicting the mean flame height of spill flames under different side wall constrains. The experimental data for different opening dimensions and side wall distances are shown to be well collapsed by this global parameter (Fig. 4) and the mean flame height with side walls can be approximated by Eq. (13).

However, as also shown in Fig. 4, there exists some dependency of λ with $\dot{Q}_{ex}^{*}$, the value of λ should be higher when $\dot{Q}_{ex}^{*}$ is larger. This will be investigated and reported in the future.

Acknowledgements

This paper was supported by National Nature Foundation of China under Grant No.51176180, National Basic Research Program of China under Grant No. 2012CB719702, Fundamental Research Funds for the Central Universities, and Program for New Century Excellent Talents in University under Grant No. NCET-09-0914.

References

[1] Yokoi, S., 1960. Trajectory of hot gas ejected from a window of a burning concrete building, Report of the Building Research Institute, Report 34.
[2] Seigel, L., 1969. The Projection of Flames from Burning Buildings, Fire Technology 5, p. 43.
[3] Thomas, P., Law, M., 1972. The Projection of Flames from Buildings on Fire, Fire Prevention Science and Technology 10, p. 19.
[4] Klopovic, S., Turan, Ö. F., 1998. Flames Venting Externally during Full-scale Flashover Fires: Two Sample Ventilation Cases, Fire Safety Journal 31, p. 117.
[5] Klopovic, S., Turan, Ö. F., 2001. A Comprehensive Study of Externally Venting Flames—Part I: Experimental Plume Characteristics for Through-draft and No-through-draft Ventilation Conditions and Repeatability, Fire Safety Journal 36, p. 99.
[6] Klopovic, S., Turan, Ö. F., 2001. A Comprehensive Study of Externally Venting Flames—: Part II: Plume Envelope and Centre-line Temperature Comparisons, Secondary Fires, Wind Effects and Smoke Management System, Fire Safety Journal 36, p. 135.
[7] He, Y., Jamieson, C., Jeary, A., Wang, J., Karlsson, B., 2008. "Effect of Computation Domain on Simulation of Small Compartment Fires," Fire Safety Science - Proceedings of the 9th International Symposium, International Association for Fire Safety Science, pp. 1365-1376.
[8] Sun, X., Hu, L., Chow, W., Xu, Y., Li, F., 2011. A Theoretical Model to Predict Plume Rise in Shaft Generated by Growing Compartment Fire, International Journal of Heat and Mass Transfer 54, p. 910.
[9] Hasemi, Y., 1984. Experimental Wall Flame Heat Transfer Correlations for the Analysis of Upward Wall Flame Spread, Fire Science and Technology 4, p. 75.
[10] Tang, F., Hu, L., Delichatsios, M., Lu, K., Zhu, W., 2011. Experimental Study on Flame Height and Temperature Profile of Buoyant Window Spill Plume from an Under-ventilated Compartment Fire, International Journal of Heat and Mass Transfer, p. 93
[11] Hu, L., Lu, K., Delichatsios, M., He, L., Tang, F., 2011. An Experimental Investigation and Statistical Characterization of Intermittent Flame Ejecting Behavior of Enclosure Fires with an Opening, Combustion and Flame, p. 101
[12] Kawagoe, K., 1958. Fire Behavior in Rooms, Japanese Ministry of. Construction, Report of Building Research Institute, Report No. 27
[13] Lee, Y. P., Delichatsios, M. A., Silcock, G., 2007. Heat fluxes and flame heights in facades from fires in enclosures of varying geometry, Proceedings of the Combustion Institute 31, p. 2521.
[14] Delichatsios, M. A., Lee, Y. P., Tofilo, P., 2009. A New Correlation for Gas Temperature inside a Burning Enclosure, Fire Safety Journal 44, p. 1003.
[15] Lee, Y. P., Delichatsios, M. A., Ohmiya, Y., 2007. "The Study for the Physics of the Outflow from the Opening of a Burning Enclosure," Proceedings of 5th International Seminar on Fire & Explosion Hazards, pp. 27.
[16] Lee, Y. P., 2006, Heat Fluxes and Flame Heights in External Facade Fires, University of Ulster, FireSERT.
[17] Coutin, M., Most, J., Delichatsios, M., Delichatsios, M., 1999. "Flame Heights in Wall Fires: Effects of Width, Confinement and Pyrolysis Length," Fire Safety Science - Proceedings of the 6th International Symposium, International Association for Fire Safety Science, pp. 729-740.
[18] Oleszkiewicz, I., 1989. Heat Transfer from a Window Fire Plume to a Building Facade. HTD-Vol. 123, Collected papers in Heat Transfer, Book No. H00526.
[19] Himoto, K., Tsuchihashi, T., Tanaka, Y., Tanaka, T., 2009. Modeling Thermal Behaviors of Window Flame Ejected from a Fire Compartment. Fire Safety Journal 44, p. 230.
[20] Ohmiya, Y., Yusa, S., Suzuki, J., Koshikawa, K., Delichatsios, M., 2003. Aerothermodynamics of fully involved enclosure fires having external flames, 4th International Seminar Fire and Explosion Hazards, pp. 121.

[21] Ohmiya, Y., Tanaka, T., and Wakamatsu, T., 1998, A Room Fire Model for Predicting Fire Spread by External Flames, Fire Science and Technology 18(1), p. 11.
[22] Ohmiya, Y., Hori, Y., Sagimori, K., Wakamatsu, T., 2000. Predictive method for properties of flame ejected from an opening incorporating excess fuel, Proceedings of the 4th Asia–Oceania Symposium on Fire Science Technology, pp. 375.
[23] JUN, Y., 2005. Temperature Profiles of Window Jet Plume. Journal Code: Y0211A 24, p. 17.
[24] Himoto, K., Tsuchihashi, T., Tanaka, Y., Tanaka, T., 2009. Modeling the Trajectory of Window Flames with Regard to Flow Attachment to the Adjacent Wall. Fire Safety Journal 44, p. 250.
[25] Nakao, T., Yanagisawa, A., Jo, A., Wakatsuki, K., Ohmiya, Y., 2007. Fire Plume Ejected from an Opening in Unconfined SpacePart 1 Experimental Outline. Fire Science and Technology 26, p. 497.
[26] Yanagisawa, A., Jo, A., Nakao, T., Wakatsuki, K., Ohmiya, Y., 2007. Fire Plume Ejected from an Opening in Unconfined SpacePart 2 Generation Limit of the External Flame. Fire Science and Technology 26, p. 505.
[27] Jo, A., Nakao, T., Yanagisawa, A., Wakatsuki, K., Ohmiya, Y., 2007. Fire Plume Ejected from an Opening in Unconfined SpacePart 3 Behavior of Fire Plume Ejected from an Opening in the Vicinity of Opposed Walls. Fire Science and Technology 26, p. 511.
[28] Lee, Y. P., Delichatsios, M., Ohmiya, Y., Wakatsuki, K., Yanagisawa, A., Goto, D., 2009. Heat Fluxes on Opposite Building Wall by Flames Emerging from an Enclosure. Proceedings of the Combustion Institute 32, p. 2551.
[29] Otsu, N., 1975. A Threshold Selection Method from Gray-level Histograms. Automatica 11, p. 285.